# Holes and magnetic textures in the two-dimensional Hubbard model

J. A. Vergés
*Instituto de Ciencia de Materiales (CSIC), Universidad Autónoma, E-28049 Madrid, Spain*

E. Louis
*Departamento de Fisica Aplicada, Universidad de Alicante, Apartado Postal 99, E-03080 Alicante, Spain*

P. S. Lomdahl
*Theoretical Division, Los Alamos National Laboratory, Los Alamos, New Mexico 87545*

F. Guinea
*Instituto de Ciencia de Materiales (CSIC), Universidad Autónoma, E-28049 Madrid, Spain*

A. R. Bishop
*Theoretical Division, Los Alamos National Laboratory, Los Alamos, New Mexico 87545*
(Received 25 June 1990)

The Hubbard model in a two-dimensional square lattice is studied within the unrestricted Hartree-Fock approximation. It is shown that a large number of self-consistent solutions exist, which correspond to possible metastable spin and charge configurations. A solution, in which the spins are coplanar and form a vortexlike pattern, is described. The solution is stable over most of the parameter range and dominates for large values of $U/t$ or at high doping. The influence of this multiplicity of solutions on the phase diagram is discussed.

## I. INTRODUCTION

Interest in the single-band, two-dimensional Hubbard model has significantly risen since the discovery of the copper oxide superconductors.[1] Although it was originally conceived as a model of magnetic systems,[2] in which the most likely behavior was either metallic or insulating,[3] the possibility that it may exhibit superconductivity has been proposed often in recent times. Extensive investigations, using a wide variety of theoretical tools, have been made, and many possible physical regimes have been proposed. It is striking that, despite the apparent simplicity of the model, so many different scenarios have been contemplated.

In the present work, we present a comprehensive study of the properties of the system as described by the Hartree-Fock (HF) approximation, in its most unrestricted form. This analysis is a first step in a systematic expansion, in which quantum fluctuations around the mean-field parameters (the charge and spin distribution) can be included. The Hartree-Fock approximation is also useful to obtain a qualitative understanding of the system *over the entire parameter range.* It includes, in an approximate way, both charge fluctuations (which play a major role in the small $U/t$ limit) and spin waves (which describe well the strong-coupling, Heisenberg, limit). In fact, it was used to analyze the possible metal-insulator transition in the model long ago .[3]

This approach has already been followed in the literature.[4–8] The main purpose of the present work is to systematize previous results, and to discuss in detail the great variety of possible solutions allowed by the HF approximation. We will make special emphasis on the role of transverse fluctuations in the staggered magnetization, which may be relevant in the strong-coupling limit. We think that the richness of solutions obtained within this scheme can be used to understand the variety of physical regimes proposed in the literature. Moreover, it also suggests the main features of the phase diagram, as a function of doping and value of $U/t$, and relates that to an underlying "frustration."

In the next section, the general aspects of the calculations are outlined. Then, in Sec. III, numerical results are presented, and the simplest structures found are classified. A detailed study of those solutions is also discussed in that section. More complicated situations are considered in Sec. IV, followed by an analysis of the resulting density of states and excitation spectrum (Sec. V). In Sec. VI the implications for the phase diagram of the system are analyzed. Finally, we discuss the main conclusions of this work, and its relation with other approaches currently being used.

## II. THE MODEL

We study the one-band Hubbard model in finite, two-dimensional clusters (up to $13\times13$ sites in size) with *open* boundary conditions. Two parameters describe the system: the value of $U/t$ and the number of electrons. The Hamiltonian is

$$\mathcal{H}=\sum_{i,j;s} tc^{\dagger}_{i,s}c_{j,s}+\sum_{i,j} U(n_{i\uparrow}-1/2)(n_{i\downarrow}-1/2)\ . \qquad (1)$$

 

The Hartree-Fock approximation searches for the ground state and other possible excited states in the subspace of wave functions that can be written as Slater determinants. It can be cast as a variational procedure that minimizes the expectation value of the energy within this subspace. A wave function that leads to at least a stationary value of the energy is characterized by the existence of a self-consistent one-electron potential, which, in turn, defines the states in the Slater determinant. Allowing for arbitrary charge and spin fluctuations at each site of the cluster, this procedure amounts to solving the following one-particle Hamiltonian:

$$\mathcal{H}=\sum_{i,j;s} t c^{\dagger}_{i,s} c_{j,s} + \text{H.c.} - \sum_{i;s,s'} \frac{U}{2} \vec{m}_i c^{\dagger}_{i,s} \vec{\sigma}_{s,s'} c_{i,s'} + \sum_i \frac{U}{2} q_i (n_{i\uparrow}+n_{i\downarrow}) + \text{c.c.} \tag{2}$$

and the self-consistency conditions

$$\vec{m}_i = \sum_{s,s'} \langle c^{\dagger}_{i,s} \vec{\sigma}_{s,s'} c_{i,s'} \rangle \ , \tag{3a}$$

$$q_i = \langle n_{i\uparrow}+n_{i\downarrow}-1 \rangle \ , \tag{3b}$$

where $\vec{\sigma}$ stands for the Pauli matrices.

These equations define the procedure to find *the Slater determinant that best approximates the ground-state energy*. Note that a common procedure used in the analysis of flux phases for the same Hamiltonian (1) first maps it into the Heisenberg Hamiltonian (using an approximation valid in the large $U/t$ limit) and, then, introduces a decoupling scheme that leads also to a Slater determinant. While the two approaches show some similarities, there are, as well, significant differences. In principle, both Slater determinants should describe the same electronic wave function. In the Hartree-Fock case, this is the straightforward consequence of the variational principle already mentioned. The procedure itself ensures that the weight of configurations with doubly occupied sites tends to zero as $U/t \rightarrow \infty$. An auxiliary step is required in the second case, to make the wave function consistent with the initial assumption of considering only the spin degrees of freedom. Thus, the two Slater determinants cannot be directly compared. On the other hand, in the large $U/t$ limit, the HF solution shows well-defined local moments at each site of the lattice. The one-electron wave functions that make up the Slater determinant can be understood in terms of an occupied lower Hubbard band. The effective hopping matrix elements for the electrons in this band are related to the overlap between the spin wave functions in neighboring sites. When their values are complex, the electronic wave functions resemble those of electrons moving in a fictitious magnetic field. Thus, the Slater determinant associated with a flux phase described by a given *fictitious* magnetic field has a close resemblance to certain solutions of the HF equations, in which the spins have twisted configurations.

The effective potential defined in Eq. (3) is the most general decoupling possible. As the interaction term in the Hubbard Hamiltonian is local, the effective field can be written as a sum of $2\times 2$ pieces that act on the two spin components at a given site. Each of those matrices can, in turn, be decomposed into a diagonal part and a traceless contribution that can be expressed in terms of the three Pauli matrices. When the magnetization has fluctuations along more than one direction in spin space, no components of the electronic spins are conserved. Calculating the electronic wave functions amounts to the diagonalization of a matrix (the effective Hamiltonian) of dimension equal to twice the number of sites in the lattice. Self-consistency is achieved by iterating the process, until the effective potential in the Hamiltonian and the one deduced from the solution are equal. The number of iterations required depends strongly on the initial conditions. Typically, the charge distribution relaxes very rapidly to the self-consistent value, while the magnetization changes more slowly from iteration to iteration. This feature is more accentuated for large values of $U/t$, in agreement with the fact that the spin stiffness tends to zero in this limit. The iteration scheme mimics, in an approximate way, the real-space dynamics of a system of charges and spins approaching equilibrium. The fact that the new values are those derived from the solution in the previous step implies that the dynamics corresponds to a strongly damped situation, with no inertial terms. In certain cases, up to 2000–3000 iterations were required.

Certain solutions, in which the magnetization exhibits transverse fluctuations, allow us to define spin currents flowing through the bonds in the lattice. Obviously, the current at each bond has the direction, in real space, defined by the bond itself. In addition, the currents are vectorial in spin space, and a separate current can be defined for each spin component. The current with spin index $i$ flowing between nearest-neighbor sites $(k,l)$ and $(m,n)$ is

$$J^i_{(k,l);(m,n)} \propto \text{Im}\left[ \sum_{j,\text{occ}} a^{j,*}_{s,k,l} \sigma^i_{s,s'} a^j_{s';m,n} \right] , \tag{4}$$

where the sum extends over all occupied one electron states, $\sigma^i$ are Pauli matrices, and the $a$'s are the amplitudes of the wave functions at each site. The index $s$ denotes the spin direction. Note that, also, a charge current may also exist, defined as $J^0_{(k,l);(m,n)} \propto \text{Im}(\sum_{j,\text{occ};s} a^{j,*}_{s;k,l} a^j_{s;m,n})$.

It is finally worth noting that the results can immediately be applied to the attractive Hubbard model, due to the exact mapping between the two Hamiltonians on a bipartite lattice. By defining new operators such that

$$\begin{aligned} \bar{c}^{\dagger}_{\uparrow i,j} &= c^{\dagger}_{\uparrow i,j} \ , \\ \bar{c}_{\uparrow i,j} &= c_{\uparrow i,j} \ , \\ \bar{c}^{\dagger}_{\downarrow i,j} &= (-1)^{(i+j)} c_{\downarrow i,j} \ , \\ \bar{c}_{\downarrow i,j} &= (-1)^{(i+j)} c^{\dagger}_{\downarrow i,j} \ , \end{aligned} \tag{5}$$

the sign of $U$ is reversed, while $t$ is unchanged in the Hamiltonian (1). Other operators of physical significance can be mapped using the above correspondence. In par-

ticular, charge is mapped into spin, and vice versa. Because of this, the chemical potential in one model is equivalent to a magnetic field in the other, and spin currents are equivalent to charge currents. Thus, our results extend, and complement, previous calculations for the attractive Hubbard model.[9]

## III. ELEMENTARY SOLUTIONS

We first consider the simplest solutions that satisfy the Hartree-Fock equations. In the absence of doping, the most stable configuration is the antiferromagnetic Néel state, for all values of $U/t$. The value of the staggered magnetization increases smoothly as a function of $U/t$. For $U/t > 2$, we find another metastable solution of the equations, in which the spins rotate by 360°, along paths that encircle the center of the cluster. This configuration resembles very closely a vortex in a planar $XY$ model, the only difference being the presence, in our case, of small charge fluctuations, which disappear in the large $U/t$ limit. Similar solutions appear for all filling factors, and will be discussed further below. We cannot rule out the possibility that they exist for even lower values of $U/t$ than the ones mentioned above, but cannot be accommodated in the clusters we study. It is worth remarking that such a configuration is very sensitive to the choice of boundary conditions. For purely topological reasons, it changes significantly the nature of the wave functions at the boundaries of the sample. In particular, a single vortex can never be accommodated for in a cluster with periodic boundary conditions. Similarly, constraints that enforce the spin configuration to approach the Néel state at the edges are incompatible with this solution.

Away from half filling, we can broadly classify the solutions into three types.

(i) *Magnetic polarons.* Here, the magnetization points along the same direction everywhere in the cluster. The extra charge is localized in regions that can be either cigar or diamond shaped.[4,9,10] These regions define a core where the magnetization is reduced. Its size increases as the value of $U/t$ diminishes; at the same time it reflects more the anisotropy of the underlying lattice. Inside the core, there are localized electronic states, whose energies lie within the original antiferromagnetic gap. Examples are shown in Fig. 1. They can be described as magnetic

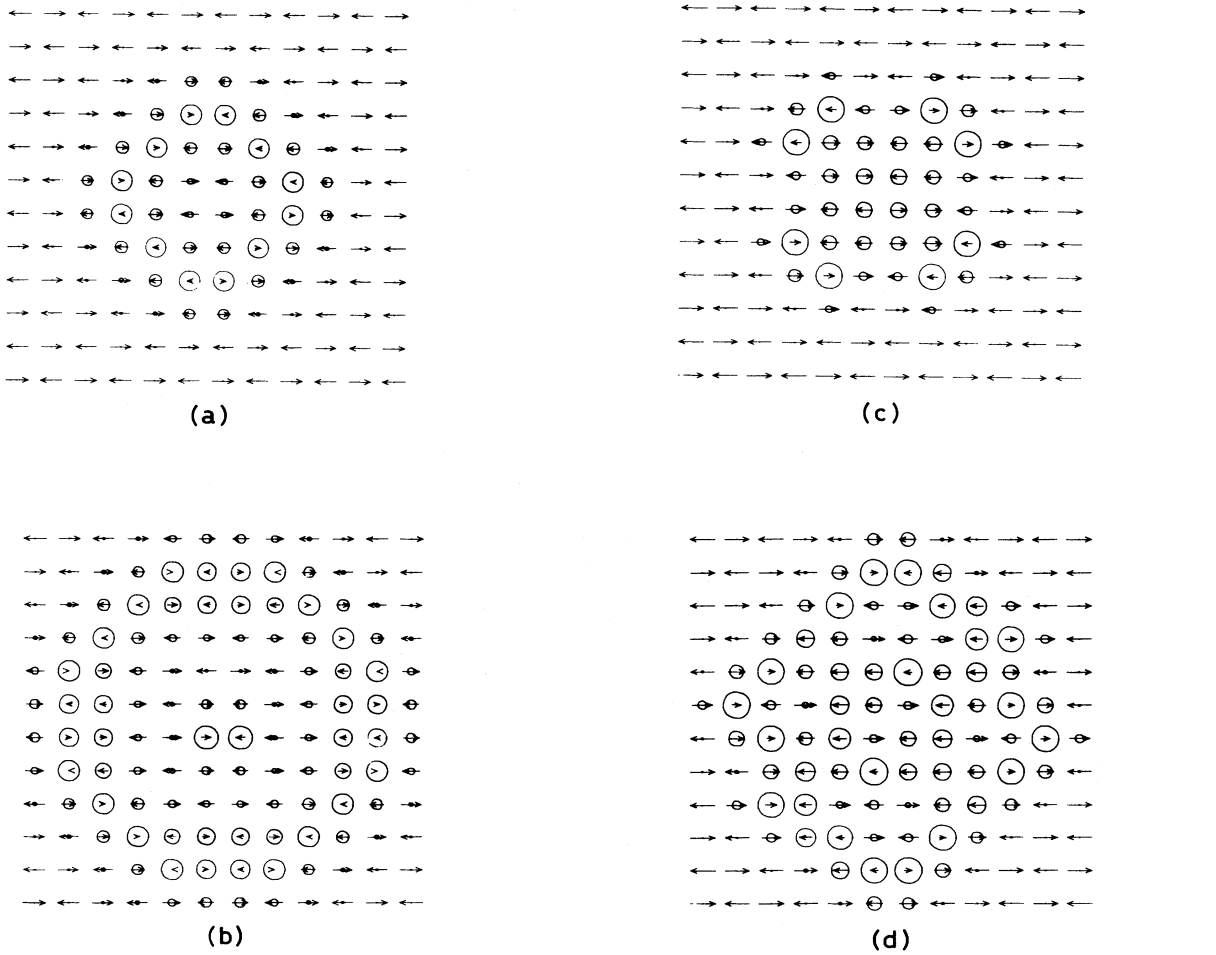


FIG. 1. Polaron solutions of the Hubbard model. (a) $U/t=5$, $n_h=12$; (b) $U/t=5$, $n_h=24$; (c) $U/t=8$, $n_h=12$; and (d) $U/t=8$, $n_h=24$. The radius of the circles at each lattice site is proportional to the total defect charge there, taken as a reference for the half-filled case. The size and direction of the arrows describe the local magnetization.

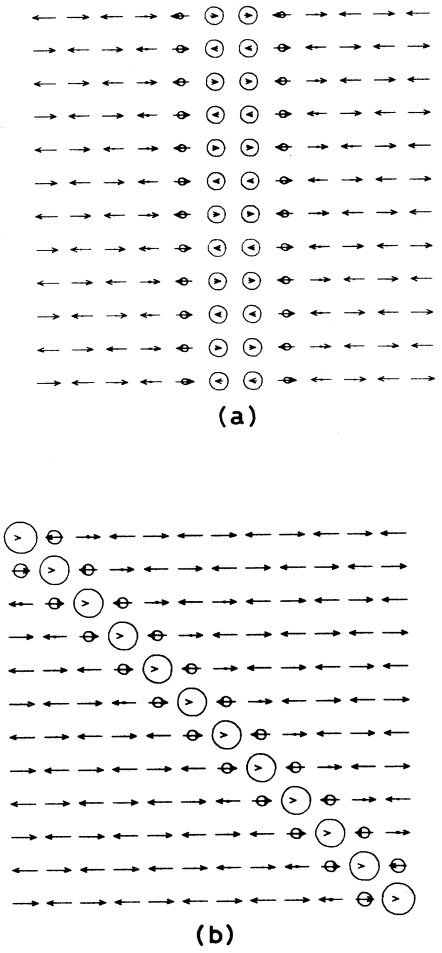


FIG. 2. Same as Fig. 1 for domain-wall solutions ($U/t=5$).

polarons, or the HF analog of the spin bag.[10]

(ii) *Domain walls.* These are linear structures that separate different domains of the reference antiferromagnetic state.[5,6] The extra electrons, or holes, are localized in them. Their width increases as the value of $U/t$ decreases. Examples are shown in Fig. 2. They are the solutions with lowest energy when the number of electrons is such that they completely fill the localized states that exist inside them. The situation resembles closely that of one-dimensional systems with degenerate ground states.

There are solutions that interpolate between (i) and (ii). As the doping increases, the polaron solution (i) evolves into a diamond-shaped bag, in which the interior has the opposite staggered magnetization from the exterior. As the size increases, this situation can be thought of as two domains, one at the center of the cluster and the other outside, separated by a domain wall and 180° out of phase. If this phase is periodically extended, it forms a superlattice.

(iii) *Vortices.* These are solutions in which the charge is localized at the center of the cluster, and the staggered magnetization rotates by 360° along paths that enclose it. As mentioned before, such solutions are metastable even in the absence of doping. As in case (i), they have a charged core, whose size and anisotropy are function of $U/t$, and a region outside where only spin waves are present. The magnetization always lies in a given plane. At the boundaries, the magnetization resembles closely that of vortices in planar antiferromagnets.

They are stable solutions for all filling levels, provided that the value of $U/t$ exceeds a certain threshold. Examples are shown in Figs. 3 and 4.

Their existence implies their stability against small deformations, which are probed by the iteration procedure followed in the calculations. This stability cannot arise from topological arguments based on the local staggered magnetization, which is a three-dimensional vector. Rather, it is due to a hidden $U(1)$ symmetry present in the problem, associated with the complex nature of the electronic wave functions.[11,12] The twist in the magnetization around the core of the defect gives rise to complex phases and spin currents. Far from the core, the electronic wave functions are similar to those of tight-binding electrons orbiting around a magnetic-flux tube. This can be better understood by using the correspondence with the attractive Hubbard model. The solutions found here are the counterparts of real vortex configurations in the superconducting phase of the negative-$U$ Hubbard model. The additional $U(1)$ symmetry, in the attractive case, describes the phase of the superconducting condensate, and the spin currents correspond to charge supercurrents in the superconductor. Following this analogy, we can assume that the gauge field associated with the $U(1)$ symmetry is proportional to the spin currents. Alternatively, we can assume the existence of a coupling term between the spin current of the additional holes and the magnetization current arising from the continuum of electronic states that build up the occupied Hubbard band.[13] This term is maximized with a finite spin current, as shown from our results.

In the case where the staggered magnetization lies in a single plane, the only nonzero current is that associated with the spin index in the normal direction ($J^z$, if the magnetization is in the $xy$ plane in spin space). Its value for the corresponding spin configurations is also shown in Fig. 3. The fact that the charge current is zero implies that the effective gauge field has an opposite sign for the two spin directions.

As in the previous cases, there are localized electronic states within the antiferromagnetic gap, where most of the extra charge resides.

The relative stability of these three types of solutions depends on $U/t$ and the filling. Figures 5 and 6 show the energies, for solutions of the three types considered above, as function of filling for $U/t=5$ and $U/t=8$. The cluster considered is $12\times12$. As the value of $U/t$ increases, vortices become more stable. The energy per particle seems to decrease smoothly for small doping, showing a tendency towards clumping.[14] In case (i) a number of holes between 4 and 8 is favored ($U/t=8$). It is hard, however, to distinguish between clumping in its strictest sense, and the influence of a residual interaction

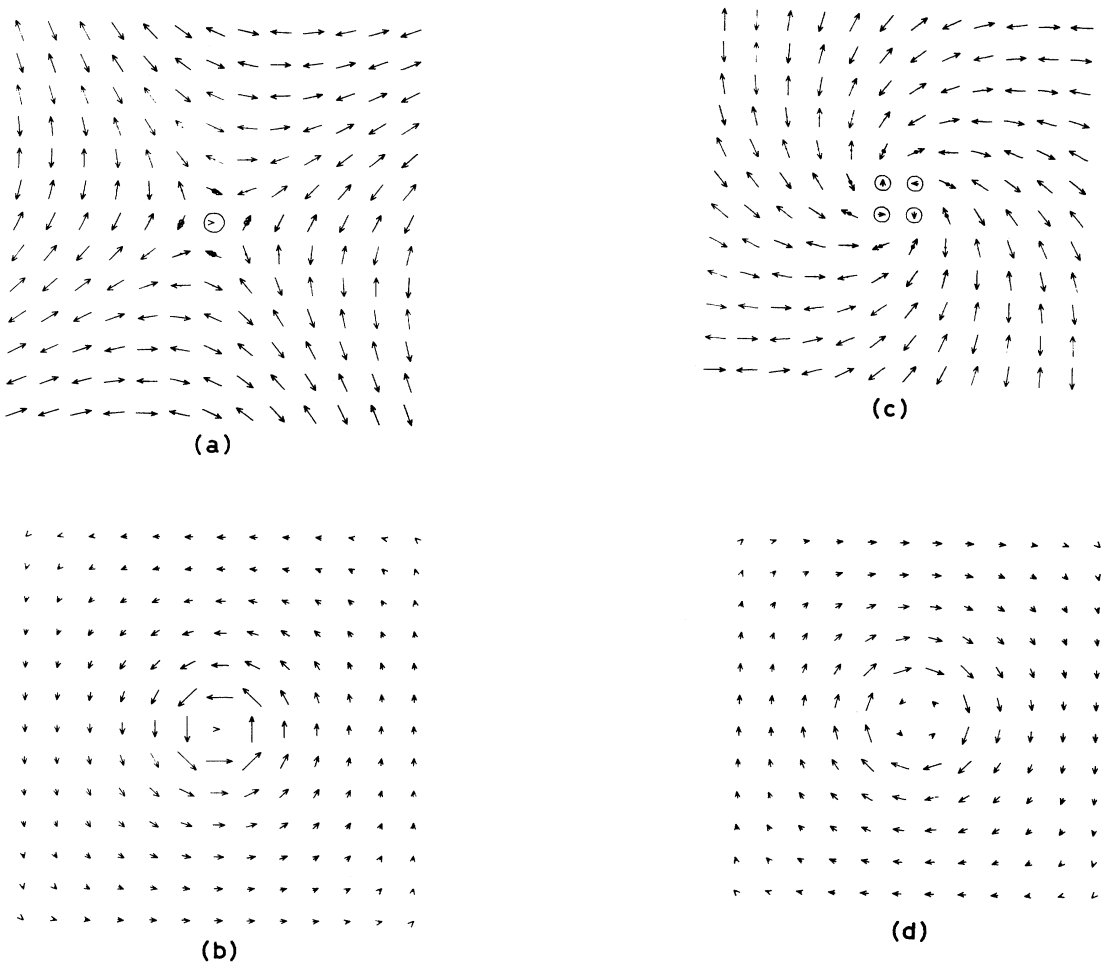


FIG. 3. Vortex solutions of the Hubbard model ($U/t=5$). $n_h=1$ [(a) and (b)] and $n_h=2$ [(c) and (d)]. (a) and (c) show the spin and charge distributions, while (b) and (d) show the spin currents.

between the elementary defects. The additional charge *is not* strongly localized, and the overall distribution suggests more strongly the existence of an ordered array of defects.

On the other hand, the energy of a vortex solution increases logarithmically as a function of cluster size. This is shown in Fig. 7. This dependence is independent of filling. Hence, it arises from the twist in the magnetization far away from the core, where the charge is localized. In that region, the system is well described in terms of spin fluctuations only, and the logarithmic dependence is a straightforward consequence of spin wave theory. It is remarkable that such a simple explanation fits so well our numerical calculations. Alternatively, we can consider the energy as arising from the kinetic energy stored in the spin currents around the core, mentioned before. In any case, this result implies that a single vortex should be unstable in large clusters, where it will be energetically favorable to split it into smaller defects. We can estimate the filling at which a vortex becomes unstable by analyzing the core contribution to the energy as a function of the number of electrons. From the results shown in the figures, vortices with two electrons seem to be favored.

It is also worth noting that, for large values of $U/t$ and small doping, solutions in which the neighborhood of the region where the hole is localized is *ferromagnetic* have also been found, in accordance with Nagaoka's theorem.[15]

## IV. OTHER SOLUTIONS

There is a large number of self-consistent solutions of the HF equations, which can be reached by the appropriate choice of initial conditions in the iteration procedure. In general, the spins either lie along a given direction or in the same plane. While some of them show very complicated magnetization patterns, most can be defined as combinations of the elementary defects described in the preceding section. Figure 8 shows different multivortex solutions. In these cases the initial distribution of magnetization was close to the final one, although the charge started uniformly distributed. Thus, a significant locali-

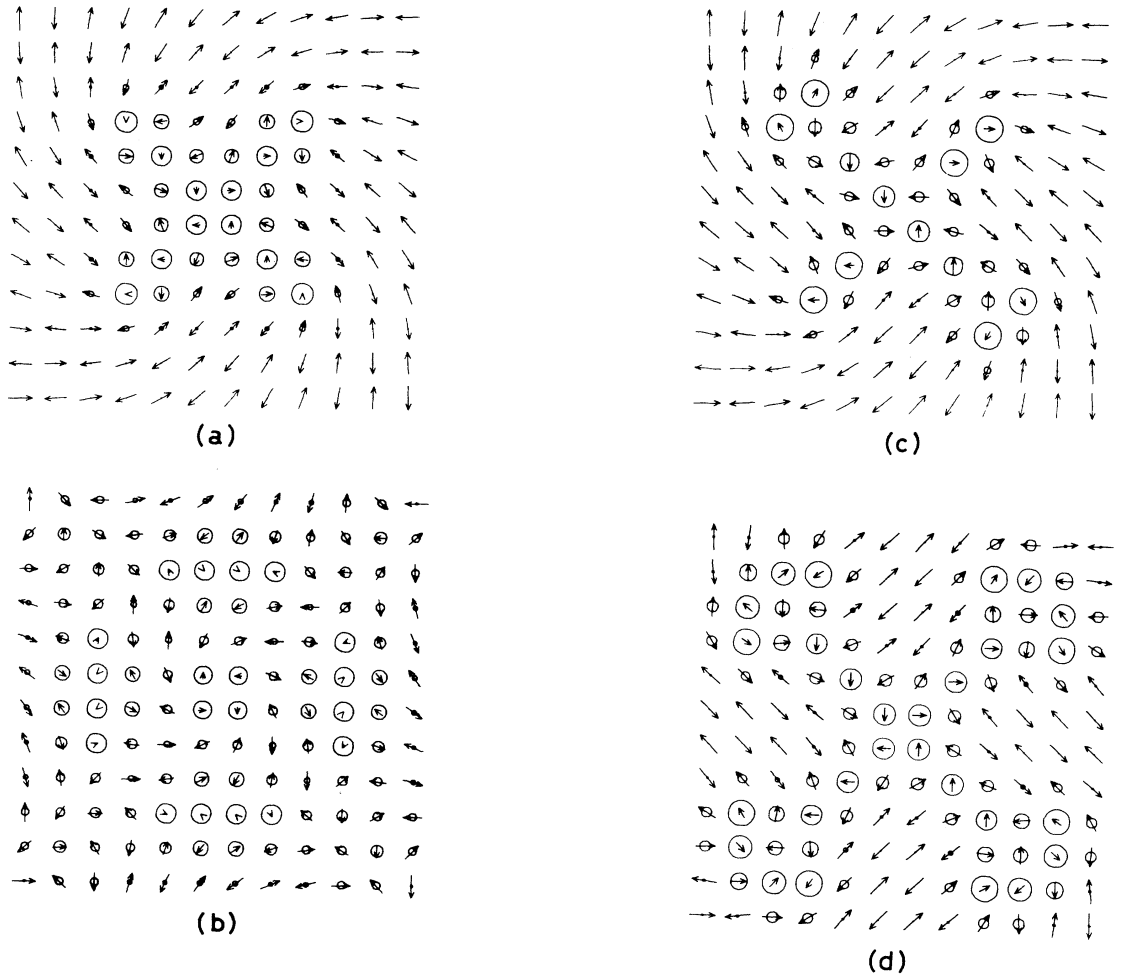


FIG. 4. Same as Fig. 1 for the vortex solutions.

zation of the charge has taken place, with the resulting appearance of electronic states within the antiferromagnetic gap. On the other hand, the position of the vortices has not changed much. We ascribe this effect to the strong pinning of the magnetization pattern to the underlying square lattice. For the large value of $U/t$ chosen, each vortex has a small core. In order for the vortex to move by one lattice spacing, the spin and charge configurations have to be significantly altered. Our results can be explained by assuming that this process requires a large cost in energy, or, in other words, that there is a Peierls-Nabarro type of energy barrier that prevents the motion of defects from site to site. Then, many local minima of the energy as a function of spin and charge distribution may exist, as evidenced from our calculations. Energetically they are nearly degenerate, and great numerical accuracy is required to find the most stable solutions.

For smaller values of $U/t$, locking effects can arise from the anisotropy of the defects themselves. In this case, the charge and spin distributions are extended, and vary little over distances compared to the lattice spacing. This makes studying them in small clusters difficult. On the other hand, they are highly anisotropic, reflecting the nesting properties of the Fermi surface in reciprocal space. This anisotropy influences the interaction between defects, and tends to give rise to locking effects into certain orientations, pinning, and to the existence of metastable minima, as before.

In general, only when the distance between vortices in the initial configuration is comparable to their core size do they change significantly in the iteration process.

It is interesting to mention that the only spin configurations that correspond to self-consistent solutions of the Hartree-Fock equations are those in which the spin directions lie either along a single direction or are coplanar. We have not found solutions where the magnetization was three dimensional in spin space. In particular, the skyrmion, which is a topologically stable configuration of the continuum Heisenberg model, does not exist for the Hubbard model in a discrete lattice. We have checked that by using it as the initial configuration in our iteration procedure. The system evolves towards a situation with a single overturned spin at the center, im-

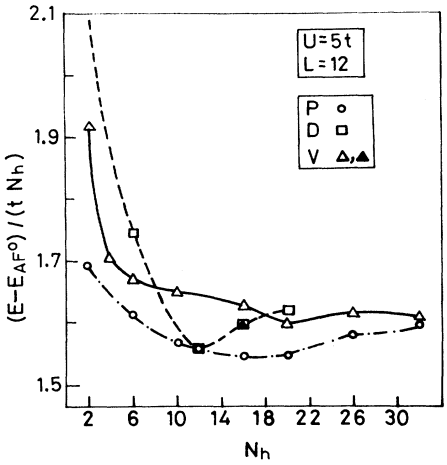


FIG. 5. Energies per additional hole for the three elementary solutions of Sec. III ($U/t=5$). Circles denote polaron solutions, squares denote domain walls, and triangles denote vortices. The solid triangles correspond to solutions with four vortices.

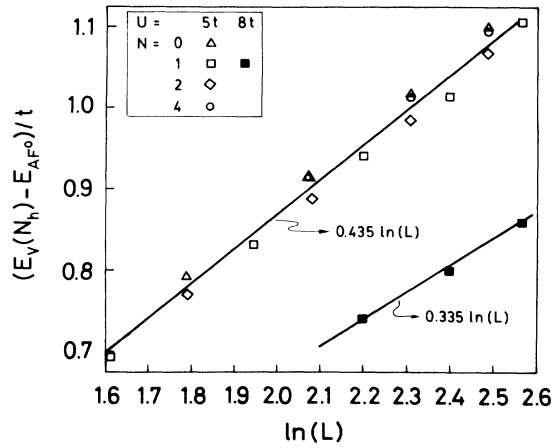


FIG. 7. Energies of vortex configurations as a function of cluster size for various fillings. The cluster sizes range from $5\times5$ to $13\times13$. A core contribution independent of size, but dependent on filling, has been subtracted. Its value is 0.29 ($n_h=0$), 1.44 ($n_h=1$), 2.78 ($n_h=2$), and 5.72 ($n_h=4$). For $U/t=8$ and $n_h=1$ the value is 2.79.

mersed in an AF background. We adscribe this collapse of the three-dimensional skyrmion to discrete-lattice effects.

The existence of many self-consistent solutions of the HF equations can also be studied analytically, in small clusters, or for periodic configurations with small unit cells. A complete classification of all Hartree-Fock solutions can be done for $2\times2$ and $3\times3$ clusters. For $n_h=2$ and $U/t>2$, the solution of lowest energy in a $2\times2$ cluster is the vortex, which resembles closely the core of the solutions discussed before. The same occurs in a $3\times3$ cluster when the total number of electrons is small. It is easy to check that the Hartree-Fock wave function obtained in this way is a very good approximation to the exact one, once the degeneracy in spin directions is taken into account. These results illustrate a general trend: for small enough clusters, vortexlike solutions are always the lowest in energy. This is very likely due to the absence of the logarithmic contribution arising from the spin distortion far from the core of the defect. As this term decreases as $U/t$ increases, this result also explains why vortex solutions are more stable at large values of $U/t$.

As mentioned before, the planar spin textures associated to vortices give rise to spin currents, which are related to the additional $U(1)$ symmetry of the model. These currents are not gauge invariant, when the phase of the wave functions is redefined, or a rotation in spin space is performed. Their curl is invariant, however. This fact implies that we can define an auxiliary vector potential in such a way that gauge-invariant quantities are related to (lattice) covariant derivatives, instead of ordinary derivatives, such as the operators used in Eq. (4) for the spin currents. This procedure is closely related to the definition of gauge-invariant quantities in terms of the phase of the superconducting condensate in the Ginzburg-Landau description of a superconductor. In an analogous way to the London equations, we can assume that our vector potential is directly proportional to the current. Then, the currents depicted in Figs. 3 and 8 can be interpreted as a visualization of this auxiliary potential. It is finally worth remarking that most of the analysis of the Hubbard model in terms of flux phases is based on the existence of the $U(1)$ symmetry discussed here, and a vector potential is defined in a similar, although not identical, way. We suggest that this reflects the fact that the underlying physics of our solutions with a twist in the transverse magnetization is very similar to that of the flux phases.

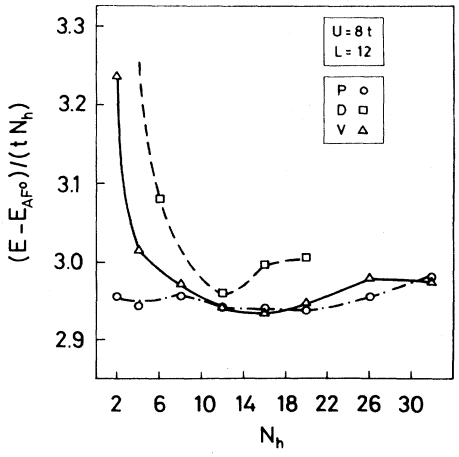


FIG. 6. Same as Fig. 4 for $U/t=8$.

## V. SINGLE-PARTICLE EXCITATIONS

The different solutions above give rise to significant differences in the excitation spectrum. A typical density

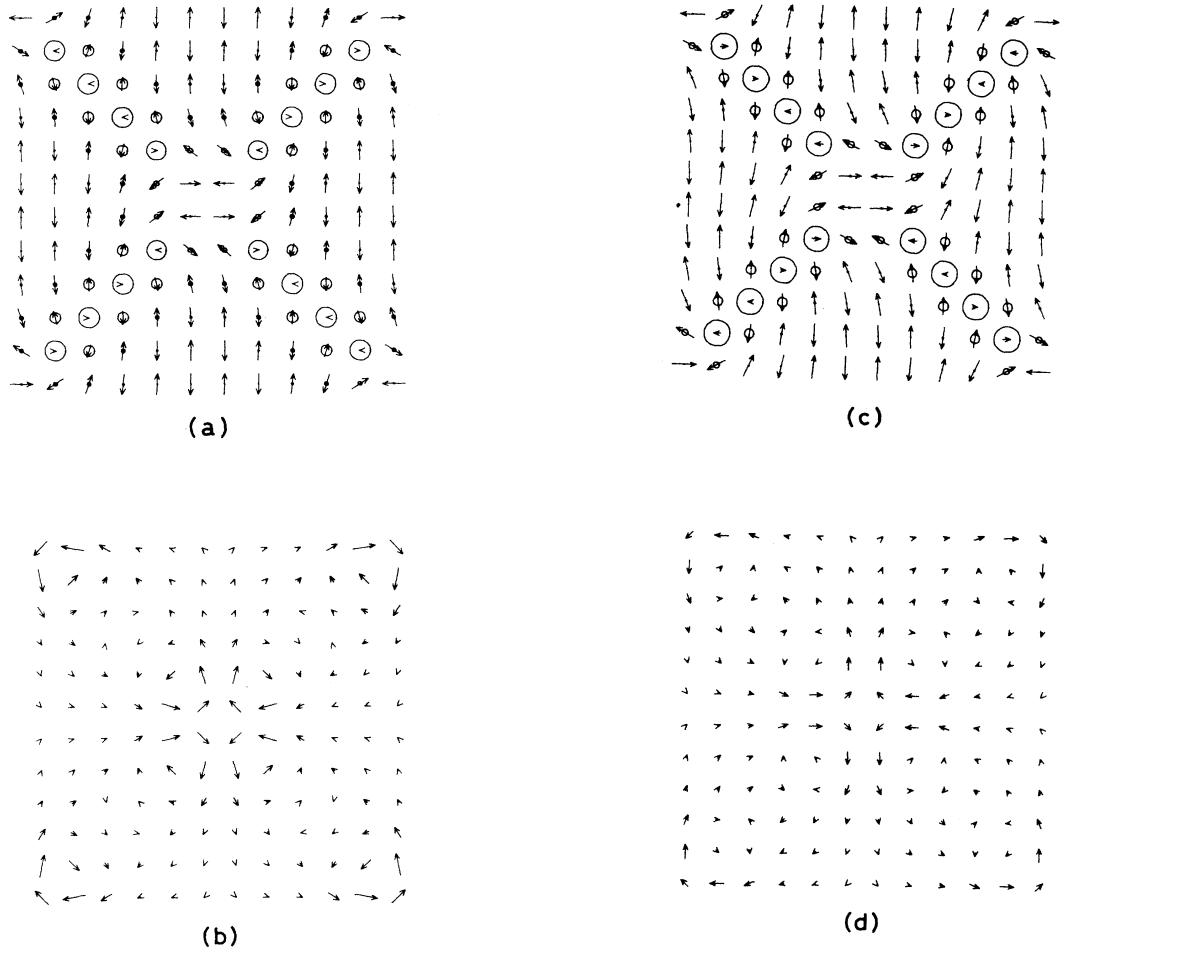


FIG. 8. Multivortex configurations for $n_h = 16$. Spin and charge configurations [(a) and (c)] and spin current distributions [(b) and (d)]. Cases (a) and (b) correspond to $U/t = 5$ and (c) and (d) to $U/t = 8$.

of states is shown in Fig. 9. The cluster size used gives a reasonable approximation to the electronic bands in the Néel state. Peaks associated with Van Hove singularities can be clearly appreciated, and the size of the antiferromagnetic gap closely follows results obtained for infinite systems.

Doping induces localized states within the gap. Fully-self-consistent solutions always have the Fermi energy close to the lower band (for holes) and it separates localized states and extended ones. Thus, the number of states in the gap adjusts itself to the degree of doping, and each new hole leads to the formation of an additional state inside the gap.

A finite small gap always remains, for all values of doping. Its magnitude depends strongly on the type of solution considered, but it is more weakly dependent on $U/t$. It is always comparable to the value of $t$.

This subgap is lowest for the vortex configuration, and highest for the domain wall, with the the polaron solution lying in between. The same trend exists for the degree of filling of the antiferromagnetic gap. While the gap edges are not altered very much upon doping, it is clear that it tends to be filled by localized states, which accommodate the extra holes. These states are more evenly spaced in the vortex configuration, while they are clustered into a narrow band for the domain wall, and the polaron shows an intermediate situation.

It is clear that higher-order corrections to the Hartree-Fock approximation depend strongly on these densities of states. Vortex solutions are, presumably, those more effective in suppressing further the local moments, and giving rise to a more disordered state. They will also influence the spin excitations, and the way in which they mix with the low-energy charge fluctuations associated with transitions across the Fermi energy.

## VI. MAIN FEATURES OF THE PHASE DIAGRAM

As mentioned before, we believe that the existence of a large number of possible self-consistent solutions to the

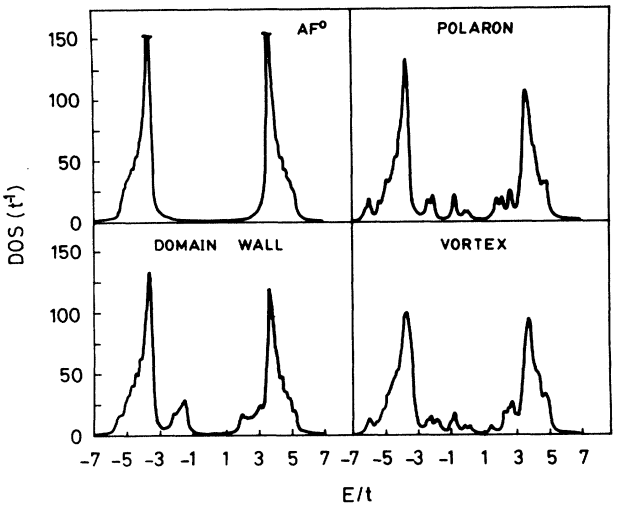


FIG. 9. Density of states (in units of $t^{-1}$) for $n_h=12$ and $U/t=8$. The three elementary configurations discussed in Sec. III are presented, as well as the reference Néel state ($n_h=0$).

Hartree-Fock equations is an intrinsic property of the two-dimensional Hubbard model near half filling. Its appearance is due to the interplay of the pinning to the lattice and the interactions between the elementary configurations. The combined effects lead to frustration, and to many metastable solutions. The same physical behavior is found in arrays of Josephson junctions in an applied field,[16] or for electrons on a lattice in an applied field.[17–19] The relative importance of these effects depends on the range of parameters considered.

(i) For small $U/t$ the elementary solutions have large and anisotopic cores. Thus, even for small doping values, they will tend to form locked patterns. The overlap of the cores can also be understood in terms of interactions mediated by charge fluctuations. The configurations that arise are, most likely, commensurate and incommensurate arrays of domain wall-like configurations. It is easy to show that either anisotropic vortices or elongated spin polarons can lead to such patterns. A particular case can be the spiral phase, already considered in the literature.[20,21]

Quantum fluctuations in the charge and spin distribution will tend to melt those phases that are less pinned to the lattice, and a liquidlike distribution of defects will replace them. Temperature can play a similar role.[22]

(ii) For large values of $U/t$, the cores of the elementary solutions are small, and there is an appreciable activation energy that prevents them from diffusing freely through the lattice. In this regime, fluctuations in the transverse components of the magnetization, away from the core, are likely to exist. Accompanying them there will be spin currents, in accordance with an analysis based on the $t$-$J$ model.[13] As mentioned before, these spin currents are associated with nontrivial phases in the electronic wave functions, which can also be interpreted in terms of a fictitious gauge field, or a spontaneous internal magnetic field.[23–26] This scenario resembles closely the flux phases proposed for the large $U/t$ limit of the Hubbard model.[11,27,18] In particular, the vortexlike solutions described in Sec. III are likely to exist. As in the $XY$ model, they interact logarithmically, and can undergo a Kosterlitz-Thouless transition. In this connection, it is interesting to note that such a liquid of excitations that interact logarithmically may have many features in common with those proposed in the *marginal-Fermi-liquid* hypothesis,[28] invoked to explain many phenomenological properties of high-$T_c$ superconductors.

(ii) Finally, we think that the most interesting regime for the existence of superconducting phases in the repulsive Hubbard model is the intermediate $U/t$ range. Then, the system cannot be viewed as in a strongly locked situation (i), or a dilute number of small defects, with low mobilities (ii). For filling factors such that the cores of the elementary defects begin to overlap, the system will be, most likely, in a liquid phase with strong interactions. One of its possible instabilities may well be towards a superfluid phase.

The analysis discussed above can be applied to charge-density-wave systems such as $BaPb_xBi_{1-x}O_3$.[29] The basic features, such as commensurability, frustration, and the existence of a strongly interacting liquid for intermediate-coupling situations, are present in this case also.

## VII. CONCLUSIONS

We have presented a comprehensive study of the solutions of the Hartree-Fock approximation for the two-dimensional repulsive Hubbard model. The most relevant feature is the existence of many nearly degenerate metastable configurations. We suggest that this is an intrinsic feature of the model, associated with frustration effects that arise from the competition between the pinning by the underlying lattice and the interactions between the elementary excitations. The influence of this competition survives in the presence of quantum fluctuations not taken into account by the Hartree-Fock approximation, although the most weakly locked configurations may be melted.

Among the possible solutions is the existence of vortex-like configurations, in which the staggered magnetization closely resembles that of a planar antiferromagnet. Their stability cannot be explained from the topology of the order parameter (a three-dimensional vector in spin space), and requires the existence of an internal $U(1)$ symmetry associated with the complex phase of the electronic wave function. In a similar way to a superconductor, spin currents arise, and a gauge field can be defined. Thus, we find, in the large $U/t$ limit, features that resemble those of certain flux phases proposed in the literature for the Hubbard model.

Finally, the frustration effects already mentioned will give rise to a complicated phase diagram. For small values of $U/t$, we expect elementary configurations with large and anisotropic cores. They lead to commensurate

and incommensurate phases, which may be locked to the underlying lattice. Some of these phases will melt, because of increased doping and/or charge fluctuations. There should be a regime, in the intermediate $U/t$ range, where the system can be best described as a strongly interacting liquid, and may be unstable towards the formation of a superconducting phase. For large values of $U/t$, our results suggest a description in terms of small vortex-like defects, with low mobilities, transverse spin fluctuations, and a fictitious internal gauge field.

Hence, we believe that the Hartree-Fock approximation suffices to give a comprehensive qualitative picture of the phase diagram of the repulsive Hubbard model, close to half filling. It is worth noting that, if the main assumptions made in this work are correct, namely the relevance of frustration effects and the existence of many nearly degenerate metastable spin and charge configurations, the analysis of the system may prove to be extremely complicated by analytical or numerical techniques.

## ACKNOWLEDGMENTS

We acknowledge financial support from CICYT (Grant No. MAT 88-0211) and the MIDAS program.

[1]J. Bednorz and K. A. Müller, Z. Phys. **64**, 189 (1986).
[2]J. Hubbard, Proc. R. Soc. (London) Ser. A **276**, 238 (1963).
[3]N. F. Mott, Philos. Mag. **20**, 1 (1969).
[4]W. P. Su, Phys. Rev. B **37**, 9904 (1988).
[5]D. Poilblanc and T. M. Rice, Phys Rev. B **39**, 9749 (1989).
[6]H. J. Schultz, Phys. Rev. Lett. **64**, 1445 (1990).
[7]J. Zaanen and O. Gunnarsson, Phys. Rev. B **40**, 7391 (1989).
[8]A. Singh and Zlatko Tesanović, Phys. Rev. B **41**, 614 (1990).
[9]A. R. Bishop, P. S. Lomdahl, J. R. Schrieffer, and S. Trugman, Phys. Rev. Lett. **61**, 2709 (1988).
[10]J. R. Schrieffer, X. G. Wen, and S. C. Zhang, Phys. Rev. Lett. **60**, 944 (1989).
[11]X. G. Wen, Phys. Rev. B **39**, 7223 (1989).
[12]A. V. Balatskii, Pis'ma Zh. Eksp. Teor. Fiz. **49**, 204 (1989) [JETP Lett. **49**, 236 (1989)].
[13]B. I. Schraiman and E. D. Siggia, Phys. Rev. Lett. **61**, 467 (1988).
[14]V. J. Emery, S. A. Kivelson, and H. Q. Lin, Phys. Rev. Lett. **64**, 475 (1990).
[15]Y. Nagaoka, Phys. Rev. **147**, 392 (1967).
[16]J. B. Marston and I. Affleck, Phys. Rev. B **39**, 11 538 (1989).
[17]S. Teitel and C. Jayaprakash, Phys. Rev. Lett. **51**, 1999 (1983).
[18]Y. Hasegawa, P. Lederer, T. M. Rice, and P. B. Wiegmann, Phys. Rev. Lett. **63**, 907 (1989).
[19]P. Lederer, D. Poilblanc, and T. M. Rice, Phys. Rev. Lett. **63**, 1519 (1989).
[20]A. Aharony, R. J. Birgenau, A. Coniglio, M. A. Kastner, and H. E. Stanley, Phys. Rev. Lett. **60**, 1330 (1988).
[21]B. I. Schraiman and E. D. Siggia, Phys. Rev. Lett. **62**, 1564 (1989).
[22]A. R. Bishop, F. Falo, and P. S. Lomdahl (unpublished).
[23]P. W. Anderson, S. John, G. Baskaran, B. Doucot, and S. D. Liang (unpublished).
[24]I. Affleck, Z. Zou, T. Hsu, and P. W. Anderson, Phys. Rev. B **38**, 745 (1988).
[25]P. A. Lee, Phys. Rev. Lett. **63**, 680 (1989).
[26]A. R. Bishop and D. Schmeltzer, Phys. Rev. B **41**, 9603 (1990).
[27]R. B. Laughlin, Phys. Rev. Lett. **60**, 2677 (1988).
[28]C. M. Varma, P. B. Littlewood, S. Schmitt-Rink, E. Abrahams, and A. E. Ruckenstein, Phys. Rev. Lett. **63**, 1996 (1989).
[29]A. W. Sleight, J. J. Gillson, and P. E. Bierstadt, Solid State Commun. **17**, 27 (1975); C. Chaillout *et al.*, *ibid.* **65**, 1363 (1988); R. J. Cava *et al.*, Nature (London) **332**, 814 (1988).